

ORIGINAL ARTICLE

Hic-5 remodeling of the stromal matrix promotes breast tumor progression

GJ Goreczny¹, JL Ouderkerk-Pecone¹, EC Olson², M Krendel¹ and CE Turner¹

The remodeling of the stromal extracellular matrix (ECM) has a crucial, but incompletely understood role during tumor progression and metastasis. Hic-5, a focal adhesion scaffold protein, has previously been implicated in tumor cell invasion, proliferation and metastasis. To investigate the role of Hic-5 in breast tumor progression *in vivo*, Hic-5^{-/-} mice were generated and crossed with the Mouse Mammary Tumor Virus-Polyoma Middle T-Antigen mouse. Tumors from the Hic-5^{-/-};PyMT mice exhibited increased latency and reduced growth, with fewer lung metastases, as compared with Hic-5^{+/-};PyMT mice. Immunohistochemical analysis showed that Hic-5 is primarily expressed in the cancer-associated fibroblasts (CAFs). Further analysis revealed that the Hic-5^{-/-};PyMT tumor stroma contains fewer CAFs and exhibits reduced ECM deposition. The remodeling of the stromal matrix by CAFs has been shown to increase tumor rigidity to indirectly regulate FAK Y397 phosphorylation in tumor cells to promote their growth and invasion. Accordingly, the Hic-5^{-/-};PyMT tumor cells exhibited a reduction in FAK Y397 phosphorylation. Isolated Hic-5^{-/-};PyMT CAFs were defective in stress fiber organization and exhibited reduced contractility. These cells also failed to efficiently deposit and organize the ECM in two and three dimensions. This, in turn, impacted three-dimensional MDA-MB-231 tumor cell migration behavior. Thus, using a new knockout mouse model, we have identified Hic-5 expression in CAFs as a key requirement for deposition and remodeling of the stromal ECM to promote non-cell autonomous breast tumor progression.

Oncogene (2017) 36, 2693–2703; doi:10.1038/onc.2016.422; published online 28 November 2016

INTRODUCTION

Normal tissue stroma is rich in fibroblasts that constantly sense the extracellular environment to regulate normal tissue homeostasis.¹ However, these fibroblasts can differentiate into cancer-associated fibroblasts (CAFs) upon receiving signals from transformed epithelial cells or through altered ECM composition.² The resulting contractile α -smooth muscle actin (SMA)-positive cells can then promote tumor cell growth through paracrine signaling, as well as protease- and force-dependent reorganization of the stromal matrix.^{3,4} The extracellular matrix (ECM) provides structural support to cells and is rich in growth factors.⁵ Furthermore, during tumor progression, linearization of the ECM fibers at the invasive front of the tumor has been suggested to facilitate tumor cell invasion into the surrounding tissue and dissemination into the bloodstream.⁶ Indeed, the density of the stromal matrix is a prognostic indicator of human breast tumors, suggesting that organization of the stroma can promote tumorigenesis.⁷ Consistent with this premise, tumor formation is elevated in a mouse model expressing a collagen I mutant that is resistant to degradation, resulting in an accumulation of stromal matrix.⁸ Furthermore, overexpression of the collagen cross-linker, lysyl oxidase, in fibroblasts can directly promote tumorigenesis and metastasis through enhanced focal adhesion signaling.⁹ Therefore, it is critical to understand the mechanisms of CAF differentiation and ECM reorganization and their role during tumor malignancy.

Focal adhesions are sites of cell adhesion to the ECM that have a key role in mechanosensing by transducing signals from the ECM

to regulate cell behavior.¹⁰ The focal adhesion scaffold/adaptor protein, Hic-5 (TGF β 1i1), is a member of the paxillin family of LIM domain proteins that has previously been implicated in skin fibroblast contractility and hypertrophic scar tissue formation.^{11,12} Although Hic-5 and paxillin share extensive homology and many of the same binding partners, they have distinct, yet overlapping functions. For example, paxillin and Hic-5 have differing roles in regulating tumor cell plasticity, as well as spatiotemporal regulation of Rac1 and RhoA activity.^{13,14} Furthermore, in contrast to paxillin^{-/-} mice, which die *in utero*,¹⁵ Hic-5^{-/-} mice, described herein are fertile and viable. Interestingly, analysis of gene expression profiles from human breast cancer patients shows Hic-5 is preferentially upregulated in the CAFs, suggesting that Hic-5 may have a crucial role in fibroblast function during tumor progression.¹⁶ Hic-5 has also been implicated in other aspects of tumor progression including epithelial to mesenchymal transition and invadopodia formation to promote cell invasion *in vitro*.^{17,18} However, the role of Hic-5 during breast tumor progression, *in vivo*, has yet to be elucidated.

To further interrogate the role of Hic-5 during breast tumor progression, we crossed the Hic-5^{-/-} mouse with the Mouse Mammary Tumor Virus-Polyoma Middle T-Antigen (MMTV-PyMT) transgenic mouse, a well-established model for human breast cancer progression.¹⁹ Importantly, although we observed no significant Hic-5 expression in the primary tumor cells, its robust expression in tumor CAFs contributed indirectly to tumor growth, invasion and metastasis through promoting the deposition and remodeling of the stromal matrix.

¹Department of Cell and Developmental Biology, State University of New York Upstate Medical University, Syracuse, NY, USA and ²Department of Neuroscience and Physiology, State University of New York Upstate Medical University, Syracuse, NY, USA. Correspondence: Dr CE Turner, Department of Cell and Developmental Biology, State University of New York Upstate Medical University, 750 East Adams Street, Syracuse 13210, NY, USA.

E-mail: turnerce@upstate.edu

Received 14 April 2016; revised 3 October 2016; accepted 3 October 2016; published online 28 November 2016

RESULTS

Hic-5 expression in the stroma is required for tumor growth

Prior to analyzing the role of Hic-5 during breast tumor progression, we evaluated whether Hic-5 is required for normal breast development. Tissue sections of mammary glands from 6-week-old Hic-5^{+/-} and Hic-5^{-/-} mice were stained for Hic-5 (Supplementary Figure 1A). Hic-5 expression was localized to myoepithelial cells (arrowhead), tissue stroma (arrow) and blood vessels (asterisk). To assess whether Hic-5 has a role in mammary gland development, whole mounts of mammary glands from 6-week-old mice were analyzed, revealing that the ducts from the Hic-5^{-/-} mice have reduced penetration into the fat pad (Supplementary Figure 1B and C). However, by 10 weeks of age, there was no significant difference in the penetration of the ducts into the fat pad (Supplementary Figure 1D and E), suggesting that although Hic-5 may have a role in the rate of normal mammary gland development, the glands are able to fully develop in the absence of Hic-5.

To determine whether the loss of Hic-5 expression impacts mammary tumor progression *in vivo*, we utilized the MMTV-PyMT mouse model. The MMTV-PyMT mouse model goes through similar stages of tumor progression as human breast cancer, including stage progression, with consistent biomarker expression, and therefore provides a widely accepted model to understand the human disease.¹⁹ To assess whether the lack of Hic-5 impacts tumor onset and growth, the tumors were monitored weekly. The onset of palpable tumor formation was slightly delayed, whereas the growth of the primary tumor was significantly reduced in the absence of Hic-5 (Figures 1a and b). We observed no significant difference in tumor latency and growth rate between the Hic-5^{+/-}; PyMT and Hic-5^{+/-}; PyMT mice (data not shown). Thus, we compared only the Hic-5^{-/-}; PyMT mice to Hic-5^{+/-}; PyMT mice throughout the study. Western blot analysis of whole tumor lysates confirmed that Hic-5 is not expressed in the Hic-5^{-/-}; PyMT tumors as compared to the Hic-5^{+/-}; PyMT tumors (Figure 1c). Furthermore, western blotting for the family member, paxillin, revealed that there was no significant change in expression in the primary tumor (Figures 1c and d). Interestingly, immunohistochemical staining of tumors from the Hic-5^{+/-}; PyMT mice revealed that Hic-5 is not significantly expressed in tumor cells (T, inset), but strong staining was observed in the surrounding CAFs within the tumor stroma (S, inset; Figure 1e). In contrast, paxillin staining was observed in both the stroma (S, inset) and in the tumor cells (T, inset; Figure 1f).

Immunofluorescence analysis of isolated CAFs revealed that Hic-5 and paxillin localize to focal adhesions (Figure 1g). Strikingly, ~45% of the Hic-5^{-/-}; PyMT CAFs exhibited a profound loss of actin toward the center of the cell, while retaining paxillin-positive focal adhesions at the periphery (Figures 1g and h). Western blotting showed that although there is a modest, albeit insignificant increase in paxillin expression in the Hic-5^{-/-}; PyMT CAFs (Figures 1i and j) it is insufficient to rescue the loss of Hic-5 function. Taken together, these data suggest that Hic-5 function in the CAFs is having an indirect, non-cell autonomous role in mammary tumor growth.

Hic-5 deficiency leads to a reduction in α -SMA-positive CAFs

Tumors have been described as wounds that never heal.²⁰ During wound healing, fibroblasts differentiate into myofibroblasts, similar to during tumor progression where the resident fibroblasts differentiate into highly contractile, α -SMA-positive CAFs.^{4,21–23} Hic-5 has previously been shown to be required for myofibroblast differentiation in dermal fibroblasts *in vitro* during wound repair.^{12,24} To determine whether genetic ablation of Hic-5 results in fewer α -SMA-positive CAFs in the tumor stroma *in vivo*, α -SMA staining was performed on Hic-5^{+/-}; PyMT and Hic-5^{-/-}; PyMT tumors sections (Figure 2a). Quantification of the area of positive staining revealed that the Hic-5^{-/-}; PyMT tumors have significantly

fewer α -SMA-positive CAFs than the heterozygotes (Figure 2b). Furthermore, α -SMA staining of isolated CAFs also showed a reduction in the number of α -SMA-positive cells derived from the Hic-5^{-/-}; PyMT tumors (Figures 2c and d). Importantly, all the cells were also vimentin positive, suggesting that the cells isolated were indeed fibroblasts (data not shown).

Previous reports have also shown that Hic-5 is required for regulating cell contractility.^{12,13,25} To assess if Hic-5 expression affects CAF contractility, a collagen gel contraction assay was performed (Figure 2e). The ability of Hic-5^{-/-}; PyMT CAFs to contract the collagen gel, in the presence of serum, was significantly reduced as compared to the control CAFs (Figure 2f). Furthermore, the relative level of phosphorylation of myosin light chain-2, a molecular readout of cellular contractility, was also significantly reduced in the Hic-5^{-/-}; PyMT CAFs (Figures 2g and h). Taken together, Hic-5 expression/function in the tumor CAFs is necessary for their differentiation and enhanced cellular contractility.

Hic-5 indirectly regulates tumor cell proliferation and signaling

Tumor volume analysis indicated that Hic-5^{-/-}; PyMT tumors grow slower than tumors in littermate controls (Figure 1b), suggesting a possible defect in tumor cell proliferation. Tumor sections were immunostained for Ki67, a proliferation marker, and EPCAM, which selectively labels epithelial cells (Figure 3a). Quantification of the percentage of Ki67 positive cells revealed that there is a more than twofold reduction in the number of proliferating tumor cells in the Hic-5^{-/-}; PyMT tumor (Figure 3b), indicating that Hic-5 deficiency in the stroma significantly reduces cellular proliferation in the tumor cells.

CAFs can indirectly regulate tumor cell growth through altered growth factor signaling and by remodeling the stromal matrix.^{2,26} For example, increased ECM density and organization has been shown to increase FAK activity in primary tumor cells, as measured by elevated Y397 phosphorylation.^{27,28} To assess whether this signaling pathway is influenced by Hic-5 expression, tumor sections from Hic-5^{+/-}; PyMT and Hic-5^{-/-}; PyMT mice were immunostained for FAK pY397 and EPCAM (Figure 3c) and the ratio of FAK pY397 fluorescence intensity to EPCAM fluorescence was quantified. The intensity of FAK pY397 in the tumor cells was significantly reduced in the Hic-5^{-/-}; PyMT sections (Figure 3d) and was also reduced in tumor lysates (Figures 3e and f). Interestingly, FAK Y397 phosphorylation was not significantly reduced in the Hic-5^{-/-}; PyMT tumor stroma or the isolated CAFs (Supplementary Figure 2A–C). Active FAK regulates multiple cellular functions including the MAPK/ERK pathway to regulate cell proliferation.²⁷ To determine whether the presence of Hic-5 in the CAFs also indirectly impacts MAPK signaling, ERK1/2 phosphorylation was assessed by western blotting (Figure 3e). Quantification of ERK1/2 phosphorylation revealed a significant reduction in the Hic-5^{-/-}; PyMT tumor lysates, as compared with the heterozygote (Figure 3g).

If Hic-5 functionally regulates stroma-tumor interactions to alter tumor growth, then we would expect to observe no effect on proliferation rates of isolated tumor cells *in vitro*. Consistent with a non-cell autonomous model of Hic-5 function, a 2,3-Bis-(2-Methoxy-4-Nitro-5-Sulphophenyl)-2H-Tetrazolium-5-Carboxanilide (XTT) proliferation assay analysis revealed no significant differences between the growth rates of the isolated Hic-5^{+/-}; PyMT and Hic-5^{-/-}; PyMT tumor cells (Figure 3h). Taken together, these findings further support a non-cell autonomous role for Hic-5 in the CAFs in promoting tumor cell growth by increasing adhesion-dependent FAK phosphorylation and MAPK activity in tumor cells.

Hic-5 expression in CAFs is required for ECM deposition and organization

CAF actively synthesizes, deposits and remodels the ECM to promote tumor growth and tumor cell invasion.⁴ Given that the

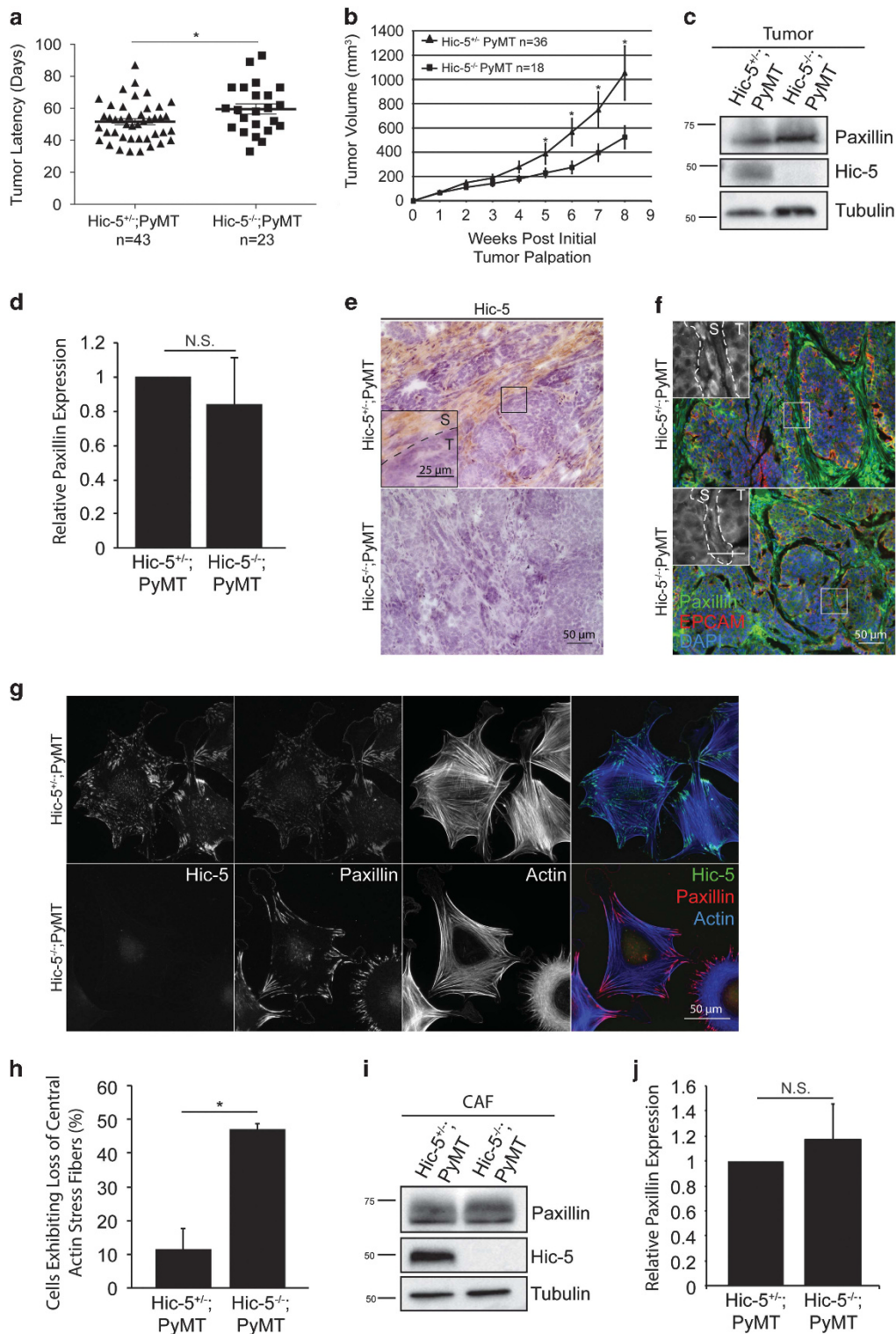


Figure 1. Hic-5 expression in the stroma is necessary for tumor growth. **(a)** Age of Hic-5^{+/+};PyMT or Hic-5^{-/-};PyMT mice when the first tumor was palpated. Average latency for Hic-5^{+/+};PyMT mice is 51.6 days and 59.6 days for the Hic-5^{-/-};PyMT mice. *n* = 43 Hic-5^{+/+};PyMT mice, *n* = 23 Hic-5^{-/-};PyMT mice. **(b)** Tumor volume is significantly reduced in the Hic-5^{-/-} mice. *n* = 36 Hic-5^{+/+};PyMT mice, *n* = 18 Hic-5^{-/-};PyMT mice. **(c)** Representative western blots of Hic-5 and paxillin staining. **(d)** Quantification of the relative paxillin expression in whole tumor lysates. *n* = 3 mice of each genotype. **(e)** Representative immunohistochemistry of Hic-5 staining in tumors from endpoint PyMT mice. The inset shows Hic-5 staining in the stroma (S), but not in the tumor cells (T). *n* = 3 mice of each genotype. **(f)** Representative paxillin staining in tumors from endpoint mice. Inset shows greyscale image of paxillin staining in the stroma (S) and the tumor cells (T). *n* = 3 mice of each genotype, scale = 25 μm. **(g)** Representative staining of Hic-5 and paxillin in isolated CAFs. *n* = 3 independent experiments. **(h)** Quantification of percentage of cells with a loss of central actin stress fibers. **(i)** Western blotting of Hic-5 and paxillin in lysates derived from the CAFs and **(j)** quantification of the relative paxillin expression. *n* = 4 independent experiments. The data represent the mean ± s.e.m., **P* < 0.05.

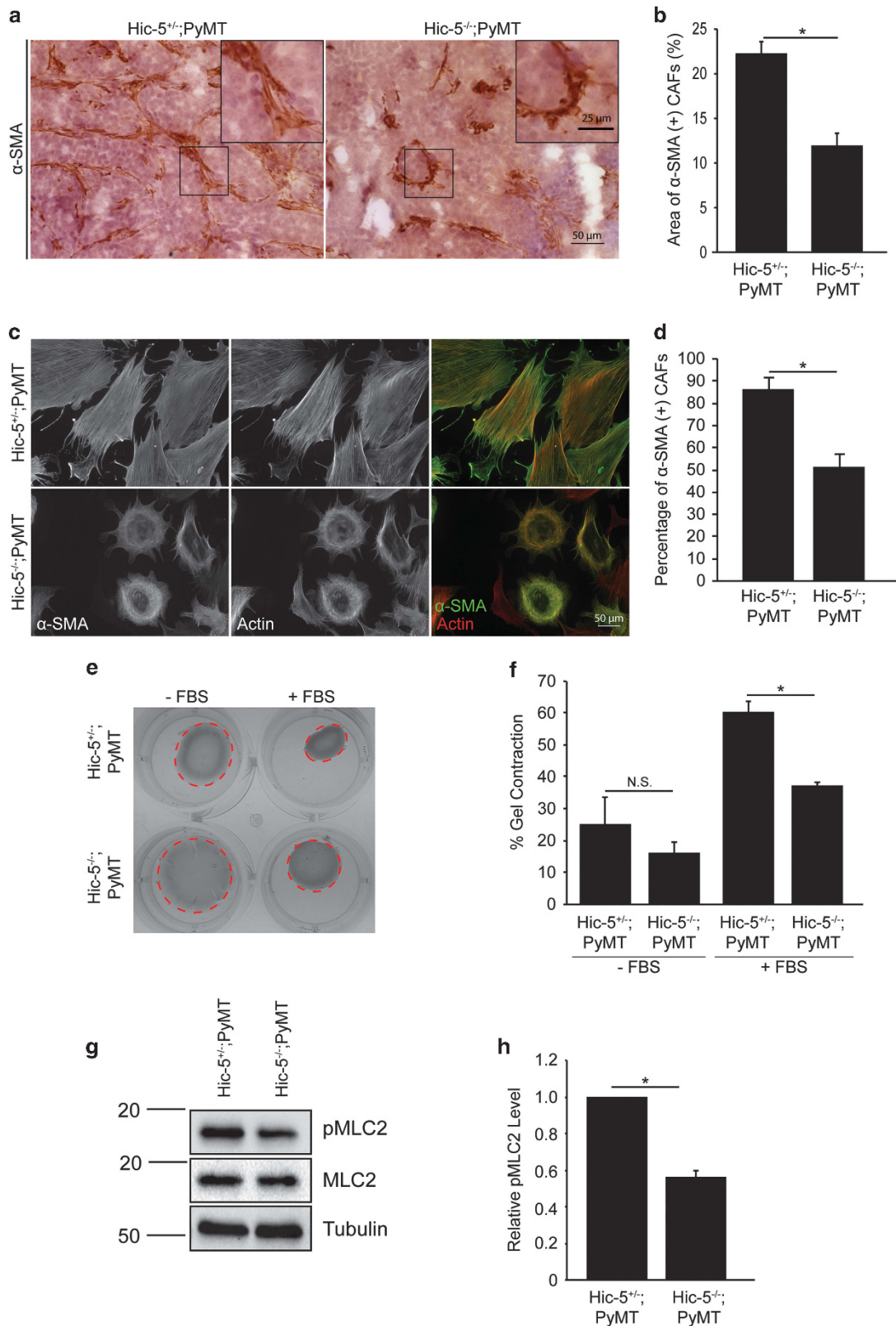


Figure 2. Hic-5 is required for CAF differentiation and contractility. **(a)** Representative sections of tumors from endpoint mice, immunostained for α-SMA (dark brown) and hematoxylin (purple). **(b)** Quantification of the area of α-SMA-positive cells. *n* = 4 mice of each genotype. The slides were blinded prior to analysis. **(c)** Isolated CAFs were stained for α-SMA and the resulting quantification **(d)** of the percentage of α-SMA-positive cells. *n* = 3 independent experiments. **(e)** Collagen gel contraction assay with Hic-5^{+/+};PyMT and Hic-5^{-/-};PyMT CAFs and subsequent quantification **(f)** of the percentage that the gel contracted. *n* = 3 independent experiments. **(g)** Western blotting for pMLC and **(h)** quantification of the relative level of MLC phosphorylation. *n* = 4 independent experiments. The data represent the mean ± s.e.m. **P* < 0.05.

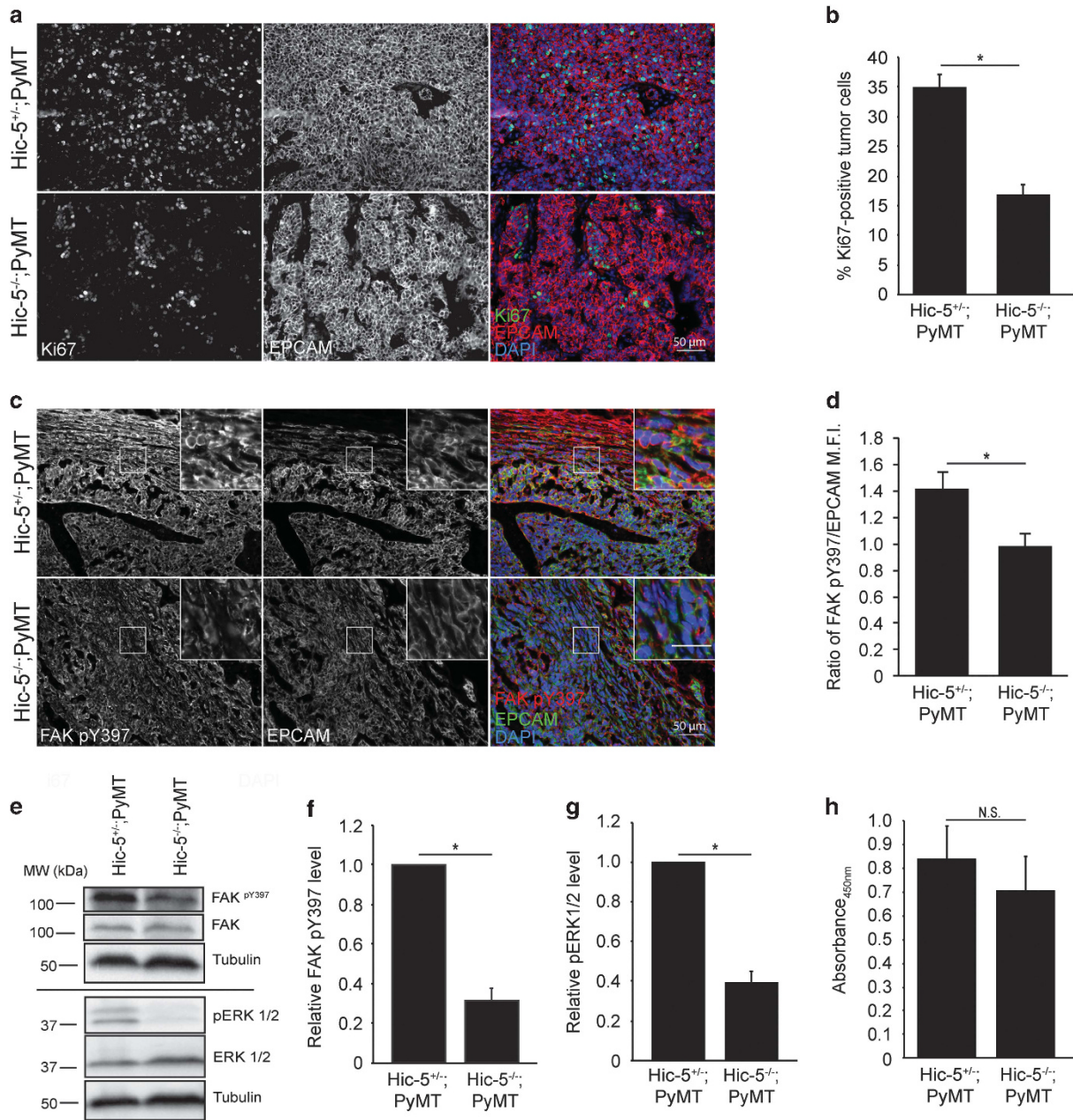


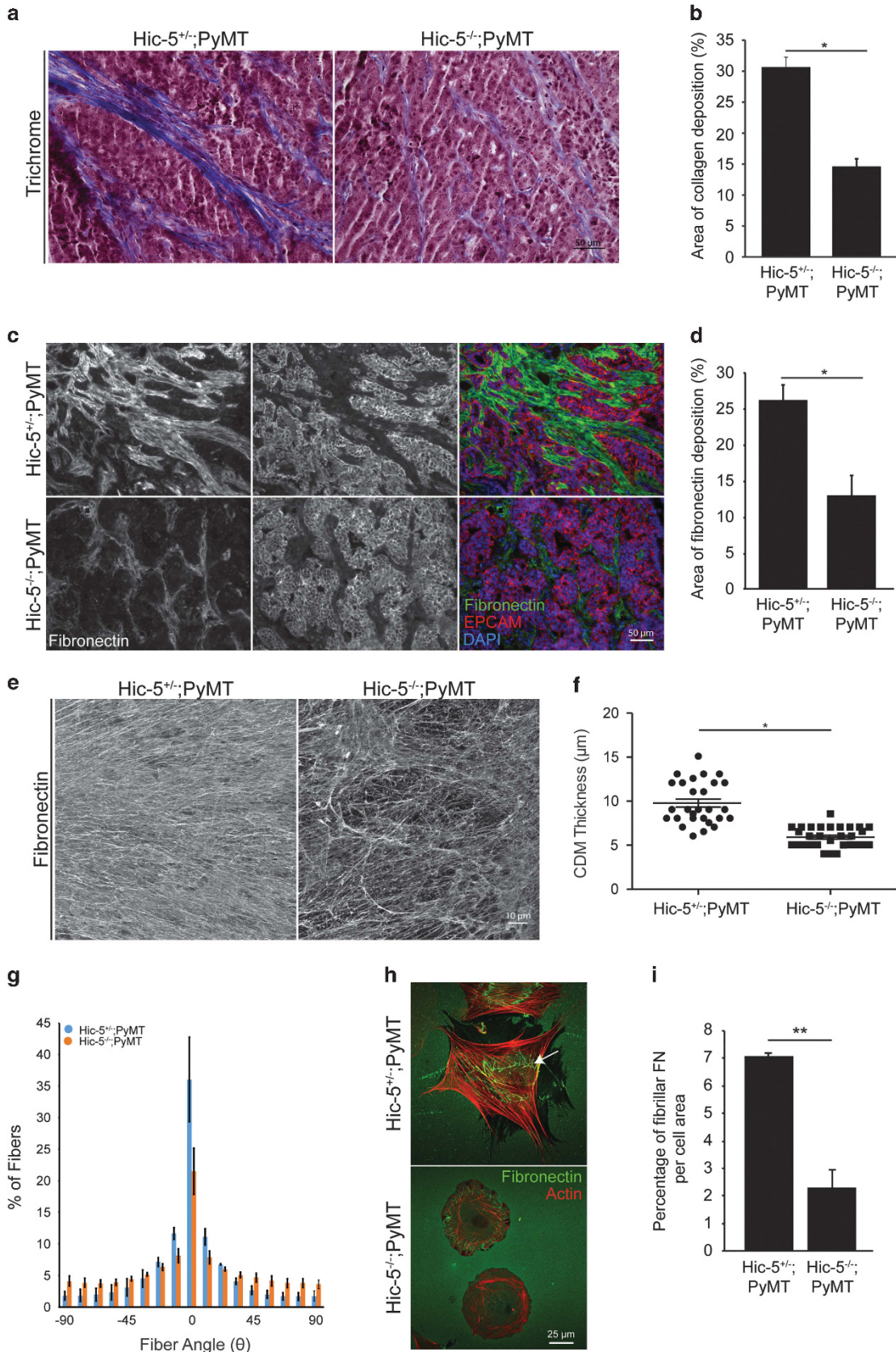
Figure 3. Hic-5 expression in CAFs indirectly regulates tumor cell growth and signaling. **(a)** Representative sections from endpoint tumors stained with Ki67. **(b)** Quantification of the percentage of Ki67 and EPCAM positive cells. $n = 4$ mice for each genotype. The slides were blinded prior to analysis. **(c)** Representative sections of endpoint tumors stained for FAK pY397 and EPCAM. The inset shows reduced FAK pY397 fluorescence intensity in the Hic-5^{-/-};PyMT tumor cells, scale = 25 μm. **(d)** Quantification of the ratio of mean fluorescence intensity (MFI) of FAK pY397 and EPCAM, $n = 3$ mice for each genotype. **(e)** Representative western blots of whole tumor lysates and subsequent quantification of **(f)** FAK pY397 and **(g)** ERK1/2 phosphorylation. $n = 3$ mice of each genotype. **(h)** Cell proliferation *in vitro* was assessed using an XTT assay. $n = 3$ independent experiments. The data represent the mean ± s.e.m. * $P < 0.05$.

Hic-5^{-/-};PyMT tumors have a reduced number of α-SMA-positive CAFs (Figures 2a-d), we assessed whether the Hic-5^{-/-};PyMT CAFs also demonstrate a reduced ability to deposit and organize the tumor ECM. Tumor sections were stained with Masson's trichrome to label fibrillar collagen (Figure 4a). Quantification of the area of positive staining showed that Hic-5^{-/-};PyMT tumors have a reduction in the total amount of fibrillar collagen (Figure 4b). In addition, the tumor sections were stained for fibronectin (Figure 4c), which was also significantly reduced in the Hic-5^{-/-};PyMT tumors (Figure 4d), suggesting that Hic-5 expression in the tumor stroma is required for matrix deposition.

Cell-derived matrices (CDMs) are 3D structures generated by fibroblasts grown at high density *in vitro* for extended periods of time.²⁹ The resulting matrix scaffolds closely resemble the composition and organization of the *in vivo* stromal microenvironment and therefore provide a useful *in vitro* system to study matrix deposition and organization and subsequently how the ECM influences tumor cell invasive behavior.^{30,31} To assess the role of Hic-5 in matrix deposition and organization, *in vitro*, we generated 3D CDMs using the isolated CAFs. Immunofluorescence staining for fibronectin showed that CDMs assembled by the Hic-5^{-/-};PyMT CAFs are less dense, with more spaces between

the fibers and of reduced thickness as compared with the CDMs generated by the heterozygote CAFs (Figures 4e and f). In addition, the angle distribution (Θ) of the fibronectin fibers was

quantified, as previously described,³¹ revealing that the fibers are more randomly oriented in the Hic-5^{-/-};PyMT CAF-derived CDMs compared with control CDMs (Figure 4g). Furthermore, the ability



of the CAFs to remodel the matrix to assemble fibronectin fibrils on a 2D substrate was also significantly reduced in the *Hic-5^{-/-}*; PyMT CAFs (Figures 4h and i). Importantly, the density of the CAF monolayers used to generate the CDMs was not significantly different between the genotypes (Supplementary Figure 3A and B). Taken together, these data indicate that *Hic-5* expression in the CAFs is required for optimal ECM deposition and organization.

Hic-5 is required to organize the matrix for optimal tumor cell migration

The reorganization of the ECM into highly aligned fibers facilitates local invasion of tumor cells into the surrounding stroma *in vivo*.⁶ To determine whether the disorganization observed in CDMs from *Hic-5^{-/-}*;PyMT CAFs impaired tumor cell migratory behavior, MDA-MB-231 cells, a highly invasive human breast cancer cell line, were plated on CDMs generated from the *Hic-5^{+/-}*;PyMT and *Hic-5^{-/-}*;PyMT CAFs (Figure 5a). MDA-MB-231 cells typically exhibit migration plasticity, undergoing frequent transitions between rounded, ameboid versus elongated, mesenchymal modes of migration.^{32,33} The percentage of cells undergoing plasticity was not significantly different between the cells migrating in the *Hic-5^{+/-}*;PyMT and *Hic-5^{-/-}*;PyMT CDMs (Figure 5b). However, we observed a higher percentage of MDA-MB-231 cells exhibiting an ameboid morphology when plated on the *Hic-5^{-/-}* CDMs (Figure 5c). This suggests that the larger gaps between fibers in the *Hic-5^{-/-}*;PyMT-generated CDMs may be more conducive to an ameboid mode of motility.

Further analysis of tumor cell behavior revealed that MDA-MB-231 cells migrating in the *Hic-5^{+/-}*;PyMT CDM moved linearly along the ECM fibers, with high directionality, whereas the MDA-MB-231 cells that were migrating in the *Hic-5^{-/-}*;PyMT CDM had reduced directionality in accordance with the reduced fiber alignment (Figures 5d and e). Interestingly, migration velocities between the MDA-MB-231 cells in the different CDMs were not significantly different (Figure 5f). Taken together, these data indicate that the *Hic-5^{-/-}*;PyMT CAFs are unable to organize the deposited matrix for optimal tumor cell invasion.

Hic-5 is required for tumor cell metastasis

The organization of the stromal matrix has also been implicated in promoting metastasis to distant organs.³⁴ As *Hic-5* is not detectable by immunostaining in tumor cells, we wanted to assess whether the presence/absence of *Hic-5* in other tissues, including the tumor stroma may still influence tumor cell invasion and metastasis. Tumor cells upregulate a basal gene program including expression of cytokeratin-14 (CK14), which serves as a useful marker of invasive cells in the primary tumor.³⁵ Accordingly, tumor sections were stained for CK14 and EPCAM (Figure 6a). The *Hic-5^{-/-}*;PyMT tumors had fewer CK14 positive tumor cells at the tumor stroma border (Figure 6b). Next, we quantified the number of circulating tumor cells (CTCs), which serves as a readout of whether the tumor cells are able to intravasate into the bloodstream. Consistent with the reduction in CK14 positive tumor cells, blood samples from the *Hic-5^{-/-}*;PyMT mice had a

significant reduction in the amount of CTCs (Figure 6c). Furthermore, the *Hic-5^{-/-}*;PyMT mouse lungs had a substantial reduction in the number of metastatic colonies (Figure 6d). Taken together, these data suggest that the microenvironment in the *Hic-5^{-/-}*;PyMT tumors is less favorable for tumor cell invasion and therefore resulting in fewer metastases, possibly owing to the reduced density and organization of the tumor stromal matrix.

DISCUSSION

In this study, we evaluated the role of *Hic-5* (TGF β 11) in breast tumor progression by crossing our recently generated constitutive *Hic-5^{-/-}* mouse with the MMTV-PyMT spontaneous breast cancer mouse model. To our knowledge, this model provides the first evidence of a role for *Hic-5* in CAF function *in vivo*, and accordingly a non-cell autonomous role for *Hic-5* in promoting tumor progression and metastasis through regulation of CAF-mediated deposition and remodeling of the tumor-associated ECM.

Stromal fibroblasts can be induced to differentiate into highly contractile CAFs, which can promote tumor growth through remodeling the ECM and/or through paracrine signaling.⁴ TGF- β signaling through the SMAD family of proteins is required for fibroblast differentiation.³⁶ Previous studies *in vitro* have implicated *Hic-5* in myofibroblast differentiation during hypertrophic scar formation through upregulation of a TGF- β autocrine loop.¹² Consistent with this study, we found that there is a reduction in the amount of α -SMA-positive CAFs in the *Hic-5^{-/-}*;PyMT tumor stroma *in vivo* (Figures 2a-d), suggesting that *Hic-5* is required for fibroblast differentiation into CAFs, possibly through its direct interactions with SMAD3 and SMAD7.^{37,38} TGF- β can also serve as a potent inducer of an epithelial to mesenchymal transition to promote tumor cell invasion.³⁹ Interestingly, *Hic-5* expression has previously been shown to be required for cultured epithelial cells to undergo a TGF- β -induced epithelial to mesenchymal transition and subsequent invadopodia formation to acquire an invasive phenotype.^{17,18} However, in the current study we did not observe detectable levels of *Hic-5* in the tumor cells, suggesting that *Hic-5* upregulation in the tumor cells is not required for invasion in this system. Further analysis into how *Hic-5* may regulate TGF- β production and activity in CAFs and tumor cells will provide mechanistic insight into how *Hic-5* may influence stromal/tumor cell crosstalk.

Mechanical feedback loops between the fibroblasts and the ECM promote normal tissue homeostasis through the regulation of intracellular contractility, to exert equal and opposing forces on the ECM.⁴⁰ However, changes in ECM density during tumor progression, or increased fibroblast contractility, can promote the upregulation of ECM gene expression, leading to the enhanced deposition and remodeling of the ECM.⁴¹⁻⁴³ Accordingly, in the absence of *Hic-5*, we observed reduced collagen and fibronectin deposition within the tumor stroma (Figures 4a-d). Furthermore, the isolated *Hic-5^{-/-}*;PyMT CAFs exhibited a loss of central focal adhesions and stress fibers (Figures 1g and h), were less contractile (Figures 2e-h) and were unable to efficiently assemble

Figure 4. *Hic-5* expression in the CAFs is required for matrix deposition and organization. (a) Representative tumor sections stained with Masson's trichrome to label fibrillar collagen. (b) Quantification of the area of collagen (blue) staining using color thresholding in ImageJ, $n = 4$ mice of each genotype. The slides were blinded prior to analysis. (c) Tumor sections stained for fibronectin and (d) quantification of the area of positive staining, $n = 3$ mice of each genotype. (e) Representative fibronectin staining of 3D-cell-derived matrices (CDMs). (f) Thickness measurements of fibronectin-stained CDMs measured using confocal microscopy. $n = 3$ independent experiments. (g) Fiber angle distribution measurements using the OrientationJ plugin for ImageJ. The angle distribution of the fibers was quantified by setting the modal angle, as defined as the angle with the highest percentage of fibers aligned, to 0° to allow direct comparison between samples. The data bars represent the percentage of fibers at the indicated angle. $n = 4$ independent experiments. (h) Representative images of CAFs plated onto fibronectin coated glass. The arrow shows fibronectin fiber organization on *Hic-5^{+/-}* CAF. (i) Quantification of the area of fibrillar fibronectin relative to the cell area. $n = 3$ independent experiments. The data represent the mean \pm s.e.m. * $P < 0.05$, ** $P < 0.005$.

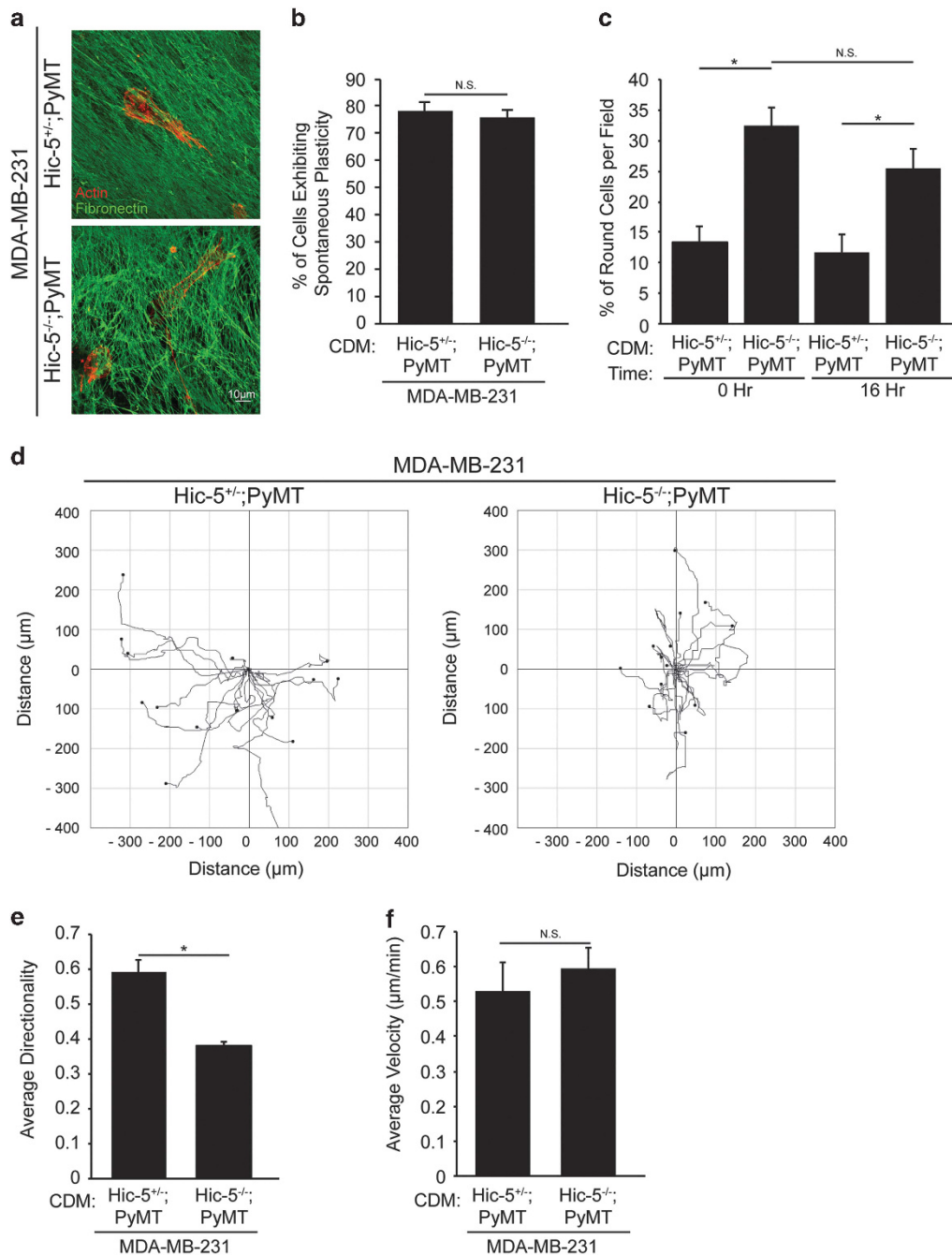


Figure 5. The Hic-5^{-/-};PyMT CDM organization influences tumor cell migration behavior. **(a)** Representative images of MDA-MB-231 cells migrating in CDMs generated from Hic-5^{+/-};PyMT and Hic-5^{-/-};PyMT CAFs stained for actin (red) and fibronectin (green). **(b)** Quantification of the percentage of cells that underwent at least one morphology change (plasticity) during the duration of the movie. **(c)** Quantification of the percentage of cells adopting a predominately round, ameboid phenotype. **(d)** Representative tracks of MDA-MB-231 cells migrating in the Hic-5^{+/-};PyMT and Hic-5^{-/-};PyMT CDMs. **(e)** Quantification of the cell directionality and **(f)** cell velocity. *n* = 4 independently performed experiments. The data represent the mean ± s.e.m. **P* < 0.05.

fibronectin fibers on their cell surface as compared with controls (Figures 4h and i). However, CAFs can also remodel the stromal matrix through force-independent mechanisms including secretion of matrix metalloproteinases, which degrade the ECM, or lysyl oxidases, promoting the crosslinking of collagen fibers and thereby contributing to increased tissue rigidity.^{9,44} Accordingly, Hic-5 has been implicated in regulating matrix metalloproteinases expression and activity in an abdominal aortic aneurysm model using an independently generated Hic-5^{-/-} mouse.⁴⁵ Thus, Hic-5

may contribute to stromal matrix organization during tumor progression via both a force-dependent mechanism involving focal adhesion maturation and stress fiber formation and through force-independent mechanisms.⁴⁶

ECM remodeling often results in a stiffer, more organized matrix that has been shown to enhance integrin-mediated signaling by increasing FAK activity to promote tumor cell growth and invasion.²⁸ It is noteworthy that the tumor cells, unlike the surrounding stroma, in the Hic-5^{-/-};PyMT tumors exhibited

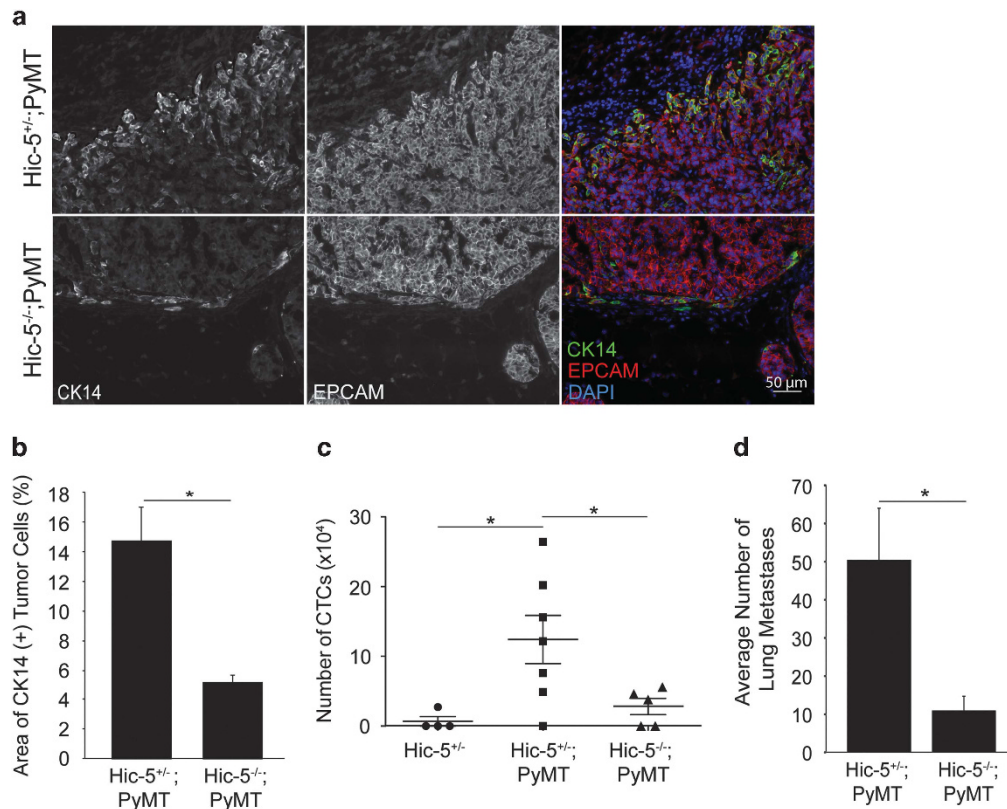


Figure 6. Mice lacking Hic-5 have reduced metastasis to the lungs. **(a)** Representative sections from Hic-5^{+/+};PyMT and Hic-5^{-/-};PyMT tumors stained for CK14 and EPCAM. **(b)** The area of CK14 staining was quantified, $n=4$ mice of each genotype. **(c)** Quantification of the number of circulating tumor cells in the blood. $n=4$ mice for Hic-5^{+/+}, $n=7$ mice for Hic-5^{+/+};PyMT and $n=5$ mice for Hic-5^{-/-};PyMT. **(d)** The total number of metastatic colonies were manually counted from sections taken every 250 μm through of the entire lung, $n=6$ mice of each genotype. The data represent the mean \pm s.e.m. * $P < 0.05$.

reduced FAK Y397 phosphorylation (Figures 3c–f) and suppressed ERK1/2 activation, which could therefore account for the reduced proliferation measured in the Hic-5^{-/-};PyMT tumor. In many cell types, Hic-5 and its homolog, paxillin, compete for FAK binding to regulate downstream effectors.⁴⁷ However, as Hic-5 is not expressed in the tumor cells, paxillin may be the predominant scaffold for FAK to regulate downstream MAPK signaling. It will be important in future studies to define the respective roles of Hic-5 and paxillin in CAFs versus tumor cells and to delineate the overlapping and distinct functions of these closely related focal adhesion proteins in breast tumorigenesis.

The Hic-5^{-/-};PyMT CAFs assembled a less dense and more disorganized 3D-CDM *in vitro* as compared to control CAFs (Figure 4e–g). Using the generated CDMs as a model to study *in vivo* matrix density and organization on tumor cell behavior, we observed that the MDA-MB-231 cells did not persistently migrate in the Hic-5^{-/-};PyMT CDM while adopting a primarily amoeboid mode of migration (Figures 5c and e).⁴⁸ We speculate that the reduction in circulating tumor cells and metastasis observed in the Hic-5^{-/-};PyMT mouse is likely due to a non-cell autonomous effect of Hic-5 expression in CAFs on tumor cell invasion (Figure 6).

Taken together, our study identifies a key role for Hic-5 in tumor malignancy through regulation of the tumor microenvironment and supports emerging findings that targeting stromal ECM composition in addition to the tumor itself may be a valid avenue for future therapeutic approaches. It will therefore be important in future studies to understand the mechanism by which Hic-5 regulates matrix synthesis and organization.

MATERIALS AND METHODS

Animals

All mouse experiments were performed in compliance with protocols approved by SUNY Upstate Medical University IACUC. Hic-5 floxed (Hic-5^{F/F}) mice were generated by the Gene Targeting and Transgenic Facility of the University of Connecticut (Farmington, CT, USA). The targeting vector was constructed such that exons 2–7 of Hic-5 Ensembl transcript, ENSMUST000000167965, were flanked with loxP sites. A Frt-PGK1-Neo-Frt-positive selection cassette was inserted 3' to exon 7. The targeting vector was introduced into 129/SvEv embryonic stem cells and homologous recombination was confirmed by G418-positive selection and Gangcylovir-negative selection. Embryonic stem cell aggregation was performed with CD1 morula and the resulting chimeric mice were screened for germline transmission of the targeting vector. The germline chimeric Hic-5^{F/F} mice were then bred to ROSA26-Flp mice to remove the PGK1-Neo cassette. The resulting Hic-5 floxed mice were then crossed to transgenic HPRT-Cre mice to generate germline deletion of exons 2–7 of Hic-5 producing the Hic-5 knockout allele. Hic-5^{+/-} mice were then maintained by backcross to C57BL/6J and intercrossed to generation homozygote mutants. The Hic-5^{-/-};PyMT mice were maintained on a mixed genetic background (C57BL/6J and FVB/N). MMTV-PyMT mice were FVB/N and were obtained from Jackson Labs (Bar Harbor, ME, USA). Mice were classified as endpoint when they either reached 14 weeks of age or when any tumor reached 2 cm³, whichever came first.

Tumor latency and growth analysis

Female mice carrying the PyMT transgene were grouped according to genotype and were palpated weekly to determine the age of tumor onset. The long and short axis of the tumors were measured weekly using digital calipers. Tumor volume was calculated using the following formula:

volume = (short axis²) × (long axis/2). Sample sizes were determined by prior experience using the PyMT mouse model.⁴⁹

Mammary gland whole mounts

Fourth inguinal mammary glands were prepared for whole mounts as previously described.⁵⁰

Tumor cell and CAF isolation

CAFs were collected as a byproduct of a tumor organoid preparation, as previously described.⁵¹ In brief, tumors were minced and incubated in digestion media (50:50 Dulbecco's Modified Eagle Medium:F12, 5% fetal bovine serum (FBS), 5 µg/ml insulin, 50 µg/ml gentamycin, 2 mg/ml collagenase, 2 mg/ml trypsin) for 30 min at 37 °C. The cells were centrifuged at 400 g for 10 min followed by incubation with 80 U of DNase. Differential centrifugation was performed to separate the single CAF cells from tumor organoids. CAFs and tumor cells were then maintained in PyMT media (50:50 Dulbecco's Modified Eagle Medium:F12 supplemented with 10% FBS, 2 mM L-glutamine, and 10 IU penicillin/10 µg/ml streptomycin), at 5% CO₂ and 37 °C. The cells were routinely tested for mycoplasma by assessing 4',6-diamidino-2-phenylindole staining.

Antibodies and reagents

Antibodies used were Hic-5, 611164; FAK, 610081; ERK1/2, 610124 (BD Biosciences, Franklin Lakes, NJ, USA); α-SMA, A2547; Fibronectin, F3648; Tubulin, T9026; 4',6-diamidino-2-phenylindole, 10236276001 (Sigma Aldrich, St Louis, MO, USA); phospho-MLC2, 3671; phospho-ERK1/2, 4307 (Cell Signaling Technologies, Danvers, MA, USA); rabbit anti-Ki67, ab15580 (Abcam, Cambridge, MA, USA); FAK pY397, 700255 (ThermoFisher, Waltham, MA, USA); paxillin, ss-5574 (Santa Cruz Biotechnology, Santa Cruz, CA, USA); Cytokeratin-14, PRB-155P (Covance, Princeton, NJ, USA); Rhodamine Phalloidin (Invitrogen, Carlsbad, CA, USA).

The EPCAM antibody, developed by AG Farr, was obtained from the Developmental Studies Hybridoma Bank, created by the NICHD of the NIH and maintained at The University of Iowa, Department of Biology, Iowa City, IA 52242.

Immunohistochemistry and immunofluorescence

Tumor sections from endpoint mice were fixed in 4% paraformaldehyde in phosphate-buffered saline (PBS), embedded in OCT and sectioned. Sections were washed in PBS and blocked in 10% normal goat serum for 2 h. Antibodies were diluted in 10% normal goat serum, washed in PBS +0.1% TX-100 (PBST), followed by incubation with secondary antibody for 2 h. The slides were washed in PBST, stained with 4',6-diamidino-2-phenylindole, and mounted. Sections were imaged using a Zeiss Axioskop2 plus microscope fitted with a Q imaging EXi Blue CCD camera using a Plan-Apochromat 20×/0.75 NA objective. Immunofluorescence staining of cells was performed as previously described.¹³

Collagen contraction assay

Bovine collagen I (Purecol, Advanced Biomatrix, San Diego, CA, USA) was mixed with 1/10th the volume of 10× MEM and brought up to pH 7.0–7.5 using 0.1 M NaOH. In total, 2 × 10⁵ Hic-5^{+/+};PyMT or Hic-5^{-/-};PyMT CAFs were embedded into a 500 µl collagen gel and polymerized at 37 °C. The collagen gels were detached from the tissue culture plastic and either serum free PyMT media or PyMT media, supplemented with 10% FBS was incubated with the gel. The percentage that the gel contracted was determined by measuring the diameter of the collagen gels before (0 h) and after (24 h) FBS addition.

CDM generation and migration analysis

Three-dimensional CDMs were generated as previously described.¹³ The thickness of the generated CDMs was measured using a Leica SP5 scanning confocal with a HCX PL APO 63×/1.40–0.60 OIL λ BL objective. The orientation of the fibronectin-stained fibers was quantified using the OrientationJ plugin for ImageJ.⁵² The modal angle, as defined as the angle that had the highest percentage of fibers oriented, was set to 0 to allow for direct comparison between images.

For migration analysis, parental MDA-MB-231 human breast cancer cells (ATCC) were seeded into the generated CDMs for 4 h in the presence of

serum. After 4 h, time lapse imaging was performed on a Nikon TE2000 microscope equipped with an environmental chamber and imaged using a HCX Plan Fluotar 10×/0.30 NA objective with images taken every 10 min for 16 h. The percentage of cells exhibiting plasticity was assessed by scoring the number of cells undergoing at least one amoeboid to mesenchymal phenotypic switch. The Manual tracking plugin in ImageJ was used to track the cell centroid over the length of the movie. The Chemotaxis and Migration plugin in ImageJ was used to calculate directionality and migration velocity.

Fibronectin-clearing assay

CAFs were plated onto 10 µg/ml fibronectin coated glass coverslips and allowed to spread/clear the fibronectin matrix for 4 h. Images of the cells were acquired using a Leica SP5 scanning confocal with a HCX PL APO 63×/1.40–0.60 OIL λ BL objective. Area of fibronectin fibers was quantified relative to the cell area using ImageJ.

XTT assay

Tumor cells were plated 24 prior to incubation with XTT reagent in a 96-well dish. The XTT reagent was mixed with phenazine methosulfate immediately before labeling cells and incubated for 2 h at 37 °C and 5% CO₂. The 450 nm absorbance was measured using a Molecular Devices Emax Precision Microplate Reader.

Isolation of circulating tumor cells

Blood was collected via cardiac puncture of endpoint mice using heparin sulfate as an anticoagulant. Red blood cells (RBCs) were lysed with RBC lysis buffer (10× stock: 150 mM NH₄Cl, 10 mM NaHCO₃, 1 mM ethylenediaminetetraacetic acid). Cells were centrifuged at 250 g for 7 min, washed in 2% FBS in PBS, and centrifuged at 50 g for 5 min. The pellet was resuspended in 500 µl PyMT media and added to an 8 µm transwell filter and centrifuged at 50 g for 1 min. The cells remaining on the filter were harvested and counted using a Biorad TC20 Automated Cell Counter with the size gated from 9–40 µm.

In vivo metastasis quantification

Lungs from endpoint mice were fixed in 10% formalin and embedded in paraffin. Ten micron sections were collected every 250 µm and stained using standard hematoxylin and eosin. The total number of lung metastases on each section were summed to determine the total number of colonies.

Statistical analysis

All data were analyzed using a two-sided Student's *t*-tests using Microsoft Excel or GraphPad Prism software. All data are generated from at least three independent mice or experiments. Statistical significance is indicated by **P* < 0.05, ***P* < 0.005. All error bars represent s.e.m.

CONFLICT OF INTEREST

The authors declare no conflict of interest.

ACKNOWLEDGEMENTS

We thank members of the Turner lab for critical reading of this manuscript and for insightful discussions. We are grateful to Ian Forsythe for the mouse genotyping and additional technical assistance. We also thank Nicholas Deakin for his assistance in isolating CTCs. This work was supported by the National Institutes of Health Grant R01 CA163296 and R01 GM047607 to CET, R01 NS066071 to ECO and CET, R01 DK083345 to MK and the Carol M Baldwin Breast Cancer Research Fund of CNY awards to CET and MK.

REFERENCES

- 1 Humphrey JD, Dufresne ER, Schwartz MA. Mechanotransduction and extracellular matrix homeostasis. *Nat Rev Mol Cell Biol* 2014; **15**: 802–812.
- 2 Kalluri R, Zeisberg M. Fibroblasts in cancer. *Nat Rev Cancer* 2006; **6**: 392–401.
- 3 Goetz JG, Minguet S, Navarro-Lerida I, Lazcano JJ, Samaniego R, Calvo E et al. Biomechanical remodeling of the microenvironment by stromal caveolin-1 favors tumor invasion and metastasis. *Cell* 2011; **146**: 148–163.

- 4 De Wever O, Demetter P, Mareel M, Bracke M. Stromal myofibroblasts are drivers of invasive cancer growth. *Int J Cancer* 2008; **23**: 2229–2238.
- 5 Cox TR, Erler JT. Remodeling and homeostasis of the extracellular matrix: implications for fibrotic diseases and cancer. *Dis Model Mech* 2011; **4**: 165–178.
- 6 Provenzano PP, Eliceiri KW, Campbell JM, Inman DR, White JG, Keely PJ. Collagen reorganization at the tumor-stromal interface facilitates local invasion. *BMC Med* 2006; **4**: 38.
- 7 Boyd NF, Martin LJ, Yaffe M J, Minkin S. Mammographic density and breast cancer risk: current understanding and future prospects. *Breast Cancer Res* 2011; **13**: 223.
- 8 Provenzano PP, Inman DR, Eliceiri KW, Knittel JG, Yan L, Reuden CT *et al*. Collagen density promotes mammary tumor initiation and progression. *BMC Med* 2008; **6**: 11.
- 9 Levental KR, Yu H, Lakins JN, Egeblad M, Erler JT, Fong SF *et al*. Matrix crosslinking forces tumor progression by enhancing Integrin Signaling. *Cell* 2009; **139**: 891–906.
- 10 Geiger B, Spatz JP, Bershadsky AD. Environmental sensing through focal adhesions. *Nat Rev Mol Cell Biol* 2009; **10**: 21–33.
- 11 Thomas SM, Hagel M, Turner CE. Characterization of a focal adhesion protein, Hic-5, that shares extensive homology with paxillin. *J Cell Science* 1999; **112**: 181–190.
- 12 Dabiri G, Tumbarello DA, Turner CE, Van de Water L. Hic-5 promotes the hypertrophic scar myofibroblast phenotype by regulating the TGF-beta1 autocrine loop. *J Invest Dermatol* 2008; **128**: 2518–2525.
- 13 Deakin NO, Turner CE. Distinct roles for paxillin and Hic-5 in regulating breast cancer cell morphology, invasion, and metastasis. *Mol Biol Cell* 2011; **22**: 327–341.
- 14 Deakin NO, Ballestrem C, Turner CE. Paxillin and Hic-5 interaction with vinculin is differentially regulated by Rac1 and RhoA. *PLoS One* 2012; **7**: e37990.
- 15 Hagel M, George EL, Klim A, Tamimi R, Opitz SL, Turner CE *et al*. The adaptor protein paxillin is essential for normal development in the mouse and is a critical transducer of fibronectin signaling. *Mol Cell Biol* 2002; **22**: 901–915.
- 16 Tchou J, Kossenkov AV, Chang L, Satija C, Herlyn M, Showe LC *et al*. Human breast cancer associated fibroblasts exhibit subtype specific gene expression profiles. *BMC Med Genomics* 2012; **5**: 39.
- 17 Tumbarello DA, Turner CE. Hic-5 contributes to epithelial-mesenchymal transformation through a RhoA / ROCK-dependent pathway. *J Cell Physiol* 2007; **211**: 736–748.
- 18 Pignatelli J, Tumbarello DA, Schmidt RP, Turner CE. Hic-5 promotes invadopodia formation and invasion during TGF- β -induced epithelial-mesenchymal transition. *J Cell Biol* 2012; **197**: 421–437.
- 19 Lin EY, Jones JG, Li P, Zhu L, Whitney KD, Muller WJ *et al*. Progression to malignancy in the polyoma middle T oncoprotein mouse breast cancer model provides a reliable model for human diseases. *Am J Pathol* 2003; **163**: 2113–2126.
- 20 Schäfer M, Werner S. Cancer as an overhealing wound: an old hypothesis revisited. *Nat Rev Mol Cell Biol* 2008; **9**: 628–638.
- 21 Martin P. Wound healing—aiming for perfect skin regeneration. *Science* 1997; **276**: 75–81.
- 22 Hinz B. Formation and function of the myofibroblast during tissue repair. *J Invest Dermatol* 2007; **127**: 526–537.
- 23 Hinz B, Phan SH, Thannickal VJ, Prunotto M, Desmouliere A, Varga J *et al*. Recent developments in myofibroblast biology: Paradigms for connective tissue remodeling. *Am J Pathol* 2012; **180**: 1340–1355.
- 24 Varney SD, Betts CB, Zheng R, Wu L, Hinz B, Zhou J *et al*. Hic-5 is required for myofibroblast differentiation by regulating mechanically dependent, MRTF-A nuclear accumulation. *J Cell Sci* 2016; **129**: 774–787.
- 25 Kim-Kaneyama JR, Suzuki W, Ichikawa K, Ohki T, Kohno Y, Sata M *et al*. Uni-axial stretching regulates intracellular localization of Hic-5 expressed in smooth-muscle cells in vivo. *J Cell Sci* 2005; **118**: 937–949.
- 26 Orimo A, Gupta PB, Sgroi DC, Arenzana-Seisdedos F, Delaunay T, Naeem R *et al*. Stromal fibroblasts present in invasive human breast carcinomas promote tumor growth and angiogenesis through elevated SDF-1/CXCL12 secretion. *Cell* 2005; **121**: 335–348.
- 27 Provenzano PP, Inman DR, Eliceiri KW, Keely PJ. Matrix density-induced mechanoregulation of breast cell phenotype, signaling and gene expression through a FAK-ERK linkage. *Oncogene* 2009; **28**: 4326–4343.
- 28 Paszek MJ, Zahir N, Johnson KR, Latkins JN, Rozenberg GI, Gefen A *et al*. Tensional homeostasis and the malignant phenotype. *Cancer Cell* 2005; **8**: 241–254.
- 29 Cukierman E, Pankov R, Stevens DR, Yamada KM. Taking cell-matrix adhesions to the third dimension. *Science* 2001; **294**: 1708–1712.
- 30 Kutys ML, Doyle AD, Yamada KM. Regulation of cell adhesion and migration by cell-derived matrices. *Exp Cell Res* 2013; **319**: 2434–2439.
- 31 Amatangelo MD, Bassi DE, Klein-Szanto AJ, Cukierman E. Stroma-derived three-dimensional matrices are necessary and sufficient to promote desmoplastic differentiation of normal fibroblasts. *Am J Pathol* 2005; **167**: 475–488.
- 32 Friedl P, Alexander S. Cancer invasion and the microenvironment: plasticity and reciprocity. *Cell* 2011; **147**: 992–1009.
- 33 Friedl P, Wolf K. Plasticity of cell migration: a multiscale tuning model. *J Cell Biol* 2010; **188**: 11–19.
- 34 Pickup MW, Mouw JK, Weaver VM. The extracellular matrix modulates the hallmarks of cancer. *EMBO Rep* 2014; **15**: 1243–1253.
- 35 Cheung KJ, Gabrielson E, Werb Z, Ewald AJ. Collective invasion in breast cancer requires a conserved basal epithelial program. *Cell* 2013; **155**: 1639–1651.
- 36 Bierie B, Moses HL. Tumor Microenvironment: TGF β : the molecular Jekyll and Hyde of cancer. *Nat Rev Cancer* 2006; **6**: 506–520.
- 37 Wang H, Song K, Krebs TL, Yang J, Danielpour D. Smad7 is inactivated through a direct physical interaction with the LIM protein Hic-5/ARA55. *Oncogene* 2008; **27**: 6791–6805.
- 38 Shola DT, Wang H, Wahdan-Alaswad R, Danielpour D. Hic-5 controls BMP4 responses in prostate cancer cells through interacting with Smads 1, 5 and 8. *Oncogene* 2012; **31**: 2480–2490.
- 39 Xu J, Lamouille S, Derynck R. TGF- β -induced epithelial to mesenchymal transition. *Cell Res* 2009; **19**: 156–172.
- 40 Kuo JC. Mechanotransduction at focal adhesions: integrating cytoskeletal mechanics in migrating cells. *J Cell Mol Med* 2013; **17**: 704–712.
- 41 Gaggioli C, Hooper S, Hidalgo-Carcedo C, Grosse R, Marshall JF, Harrington K *et al*. Fibroblast-led collective invasion of carcinoma cells with differing roles for RhoGTPases in leading and following cells. *Nat Cell Biol* 2007; **9**: 1392–1400.
- 42 Cirri P, Chiarugi P. Cancer associated fibroblasts: the dark side of the coin. *Am J Cancer Res* 2011; **1**: 482–497.
- 43 Lu P, Weaver VM, Werb Z. The extracellular matrix: a dynamic niche in cancer progression. *J Cell Biol* 2012; **196**: 395–406.
- 44 Egeblad M, Werb Z. New functions for the matrix metalloproteinases in cancer progression. *Nat Rev Cancer* 2002; **2**: 161–174.
- 45 Lei XF, Kim-Kaneyama JR, Arita-Okubo S, Offermanns S, Itabe H, Miyazaki T *et al*. Identification of Hic-5 as a novel scaffold for the MKK4/p54 JNK pathway in the development of abdominal aortic aneurysms. *J Am Heart Assoc* 2014; **3**: e000747.
- 46 Burridge K, Guilluy C. Focal adhesions, stress fibers and mechanical tension. *Exp Cell Res* 2016; **343**: 14–20.
- 47 Nishiya N, Tachibana K, Shibamura M, Mashimo JI, Nose K. Hic-5-reduced cell spreading on fibronectin: competitive effects between paxillin and Hic-5 through interaction with focal adhesion kinase. *Mol Cell Biol* 2001; **21**: 5332–5345.
- 48 Petrie RJ, Doyle AD, Yamada KM. Random versus directionally persistent cell migration. *Nat Rev Mol Cell Biol* 2009; **10**: 538–549.
- 49 Ouderkerk-Pecone JL, Goreczny GJ, Chase SE, Tatum AH, Turner CE, Krendel M. Myosin 1e promotes breast cancer malignancy by enhancing tumor cell proliferation and stimulating tumor cell de-differentiation. *Oncotarget*; e-pub ahead of print 17 June 2016; doi:10.18632/oncotarget.10139.
- 50 Plante I, Stewart MK, Laird DW. Evaluation of mammary gland development and function in mouse models. *JoVE* 2011; **53**: pii: 2828.
- 51 Nguyen-Ngoc KV, Shamir ER, Huebner RJ, Beck JN, Cheung KJ, Ewald AJ. 3D culture assays of murine mammary branching morphogenesis and epithelial invasion. *Methods Mol Biol* 2015; **1189**: 135–162.
- 52 Rezakhanli R, Agianniotis A, Schrauwen JT, Griffa A, Sage D, Bouten CV *et al*. Experimental investigation of collagen waviness and orientation in the arterial adventitia using confocal laser scanning microscopy. *Biomech Model Mechanobiol* 2012; **11**: 461–473.

Supplementary Information accompanies this paper on the Oncogene website (<http://www.nature.com/onc>)